SIAM J. APPL. MATH.
Vol. 82, No. 3, pp. 1068–1090

PARAMETRIC RESONANCE FOR ENHANCING THE RATE OF METASTABLE TRANSITION*

YING CHAO† AND MOLEI TAO‡

Abstract. This work is devoted to quantifying how periodic perturbation can change the rate of metastable transition in stochastic mechanical systems with weak noises. A closed-form explicit expression for approximating the rate change is provided, and the corresponding transition mechanism can also be approximated. Unlike the majority of existing relevant works, these results apply to kinetic Langevin equations with high-dimensional potentials and nonlinear perturbations. They are obtained based on a higher-order Hamiltonian formalism and perturbation analysis for the Freidlin–Wentzell action functional. This tool allowed us to show that parametric excitation at a resonant frequency can significantly enhance the rate of metastable transitions. Numerical experiments for both low-dimensional toy models and a molecular cluster are also provided. For the latter, we show that vibrating a material appropriately can help heal its defect, and our theory provides the appropriate vibration.

Key words. metastable transition, Freidlin–Wentzell action functional, nonautonomous rare event, parametric resonance, material defect

AMS subject classifications. 60H10, 37J50, 37J45

DOI. 10.1137/21M144966X

1. Introduction.

Rare but reactive dynamical events induced by small noise underlie many physical, chemical, and biological problems. Examples of such rare events include climate changes (e.g., [43]), nucleation in phase transitions (e.g., [26]), activated chemical reactions, and conformation switching of macromolecules (e.g., [55]). To explore the mechanism of rare transition in stochastic dynamical systems is a challenging task. In the limit of weak noise, Freidlin–Wentzell large deviation theory [20, 14] provides a framework for assessing the likelihoods of those rare events.

This paper considers a specific case of nonautonomously forced stochastic mechanical system, modeled as a second-order[1] and underdamped kinetic Langevin system, perturbed by a τ_f-periodic in t force $f(x,t)$:

$$\begin{aligned} dx &= v dt, \\ dv &= -\Gamma v dt - \nabla V(x) dt + \varepsilon f(x,t) dt + \sqrt{\mu}\Gamma^{\frac{1}{2}} dW. \end{aligned} \tag{1.1}$$

Here variables $x, v \in \mathbb{R}^{nd}$ denote the configuration and velocity of n particles in $\mathbb{R}^d$, respectively, $V : \mathbb{R}^{nd} \to \mathbb{R}$ is the potential, $\Gamma \in \mathbb{R}^{nd\times nd}$ is a symmetric positive definite damping coefficient matrix, and W is an nd-dimensional Wiener process.

*Received by the editors October 12, 2021; accepted for publication (in revised form) March 7, 2022; published electronically June 23, 2022.
https://doi.org/10.1137/21M144966X
Funding: This work was supported by the NSFC through grant 12101484 and by the NSF through grant DMS-1847802.

†School of Mathematics and Statistics, Xi'an Jiaotong University, Xi'an, Shaanxi 710049, People's Republic of China (yingchao1993@xjtu.edu.cn).
‡School of Mathematics, Georgia Institute of Technology, Atlanta, GA 30332 USA (mtao@gatech.edu).

[1]We call it second order because it can be formally written as $\ddot{x} + \Gamma\dot{x} = -\nabla V(x) + \varepsilon f(x,t) + \sqrt{\mu}\Gamma^{\frac{1}{2}}\xi(t)$, which should be compared with the first order system of perturbed overdamped Langevin, i.e., $\dot{x} = -\nabla V(x) + \varepsilon f(x,t) + \sqrt{\mu}\xi(t)$. Here, $\xi(t)$ is a standard white noise in $\mathbb{R}^{nd}$.

In (1.1), the perturbation parameter ε controls the intensity of the periodic forcing and is assumed without loss of generality to be positive. We assume μ is smaller than ε so that we first have a large deviation principle and then asymptotic analysis of the maximum likelihood path (which will be clarified in the next paragraph). We also assume $\varepsilon > 0$ is small enough so that in the absence of noise, i.e., $\mu = 0$, there exists at least two stable periodic states $x_a^\varepsilon(t)$ and $x_b^\varepsilon(t)$, separated by an unstable one $x_u^\varepsilon(t)$, bifurcated out of two local minima and a saddle of $V(\cdot)$ in the no-forcing case (i.e., $\varepsilon = 0$), for which we also assume the saddle is an attractor on the separatrix between the basins of attraction of the two minima. Note the existence of such periodic orbits is guaranteed for small enough ε due to implicit function theorem (e.g., [39]).

It is known that the presence of noise (i.e., $\mu \neq 0$) introduces a mechanism of transition between periodic solutions of the noiseless system; see, e.g., [20, 50, 34] for autonomous problems. This article considers how a time-dependent forcing $f(x,t)$ can change the transition rate, which could be understood intuitively as the likelihood of jumping from one basin of attraction to another, and this likelihood is characterized by the transition between the stable periodic states $x_a^\varepsilon(t) \to x_b^\varepsilon(t)$, which is impossible without the noise and thus termed as the "metastable transition." To quantify such transitions, which involve infinite loopings around $x_a^\varepsilon(t)$ and $x_b^\varepsilon(t)$ as $t \to \pm\infty$, it is important to specify the boundary conditions of the transition $x(t)$. Based on knowledge of infinite-time metastable transition in autonomous systems, it might be tempting to consider boundary conditions $\lim_{t\to-\infty} x(t) - x_a^\varepsilon(t) = 0$ and $\lim_{t\to+\infty} x(t) - x_b^\varepsilon(t) = 0$, but we will actually allow an additional phase difference, whose ramification will be detailed later on.

More precisely, let $\|\cdot\|_B$ denote a weighted norm, $\|x\|_B = \sqrt{x^T B x}$, where $x \in \mathbb{R}^{nd}$ and $B \in \mathbb{R}^{nd\times nd}$ is a positive definite matrix. Given an autonomous problem

$$\begin{aligned} dx &= v\,dt, \\ dv &= -\Gamma v\,dt - \nabla V(x)\,dt + \sqrt{\mu}\Gamma^{\frac{1}{2}}\,dW, \end{aligned} \tag{1.2}$$

equipped with boundary condition $x(T_1) = x_1$ and $x(T_2) = x_2$, Freidlin–Wentzell large deviation theory gives that, as $\mu \to 0$, the probability density of having a solution $x(\cdot)$ is formally asymptotically equivalent to $\exp\{-S_{T_1,T_2}[x]/\mu\}$, where the associated action functional $S_{T_1,T_2}[x]$ is given by

$$S_{T_1,T_2}[x] = \begin{cases} \frac{1}{2}\int_{T_1}^{T_2} \|\ddot{x} + \Gamma\dot{x} + \nabla V(x)\|_{\Gamma^{-1}}^2 dt, & x \in \bar{C}_{x_1}^{x_2}(T_1,T_2), \\ \infty, & \text{otherwise}, \end{cases}$$

where $\bar{C}_{x_1}^{x_2}(T_1,T_2)$ denotes the space of absolutely continuous functions in $[T_1,T_2]$ that satisfy $x(T_1) = x_1$ and $x(T_2) = x_2$.

The nonautonomy of (1.1) creates extra challenges. To the best of our knowledge, a rigorous probabilistic theory that estimates the transition rate for nonautonomous periodically driven systems is still lacking. Nonetheless, based on the results of existing research in physics (e.g., [17, 47, 16]) and numerical evidences (e.g., [10]), it makes sense that in the $\mu \to 0$ limit, the transition rate (this time between metastable periodic orbits in system (1.1) instead of metastable fixed points in system (1.2)) can be essentially characterized by $\exp(-S^\varepsilon/\mu)$, where the quantity S^ε is described as follows:

$$\begin{aligned} S^\varepsilon &= \inf_{x\in\bar{C}_{x_1}^{x_2}(\mathbb{R}),\lim_{t\to-\infty} x(t)-x_a^\varepsilon(t)=0,\lim_{t\to+\infty} x(t)-x_b^\varepsilon(t)=0} S^\varepsilon[x(t)], \\ S^\varepsilon[x(t)] &= \frac{1}{2}\int_{-\infty}^{+\infty} \|\ddot{x} + \Gamma\dot{x} + \nabla V(x) - \varepsilon f(x,t)\|_{\Gamma^{-1}}^2 dt. \end{aligned} \tag{1.3}$$

Here the minimization in (1.3) is performed in the space of absolutely continuous functions in $\mathbb{R}$. We remark that the usage of boundary conditions at $\pm\infty$ is reasonable, as the minimum in (1.3) is generally achieved when $T_2 - T_1 \to \infty$. In other words, maximum likelihood transition time between two metastable periodic states is infinite (e.g., [25]). In most parts of this article, we will be only concerned with local minimizers of $S^\varepsilon[x(t)]$. The reason is that convexity is not guaranteed and global minimization might be too difficult. We call these minimizers maximum likelihood paths (MLPs) throughout this paper (they are also called instantons in the physical literature). Since we will be considering just local minimizers, assume without loss of generality that there is only one $x_u^\varepsilon(t)$, as we will be just considering transitions through its neighborhood.

In the absence of a nonautonomous forcing ($\varepsilon = 0$), hopping between metastable states of the kinetic Langevin equation has been studied in detail, including the characterization of MLPs and the corresponding action value. For example, Souza and Tao [48] analyzed minimizers of the Freidlin–Wentzell action for the kinetic Langevin equation with respect to various types of friction coefficients for illustrating features in kinetic Langevin metastable transitions that markedly differ from the familiar overdamped picture. The idea studied in this paper is to use specific periodic perturbations ($\varepsilon \neq 0$) to facilitate metastable transitions. This idea is inspired, for example, by the investigation of periodically perturbed Markov jump processes in chemical and epidemiological applications [18, 2, 4], by stochastic resonance [42, 28, 21, 36], by the use of nongradient forcing (which can be interpreted as an irreversible component, just like how time-dependent perturbation can also be interpreted so) for changing transition rate [26], and by many successes in controlling deterministic systems using periodic perturbations [29, 41, 45, 46, 27, 3, 13, 6, 32, 31, 52, 49, 57]. To quantify how periodic perturbation can change the rate of metastable transition, a key practical question then becomes how to compute the minimum of the Freidlin–Wentzell action.

Continuous and significant efforts have already been made to understand noise-induced transitions or escapes in the presence of a periodic driving. Smelyanskiy et al. [47] and Dykman et al. [16] proved that the escape probabilities can be changed very strongly even by a comparatively weak force. Agudov, Spagnolo, and Agudov[1, 15] studied the effect of noise-enhanced stability of periodically driven metastable states. Chen et al. [9] identified a most likely noise-induced transition path under periodic forcing in the framework of finite noise. However, these works mainly have been focused on first-order systems, many of which may be viewed as the overdamped limits of second-order systems.[2] Meanwhile, seminal results on the noise-activated escape rate of a second-order and under-damped dynamical system exist [17, 37], although they mostly considered only the case of a single particle and linear additive driving forcing, i.e., $f(x,t) = f(t)$. It is our goal to extend the existent approaches and study the rate of metastable transition in the multiparticle/higher-dimensional systems (1.1), which have potential applications in, for instance, molecules dynamics (an example of healing material defeat, which is important in material sciences, will be provided in section 4). We also consider more general nonlinear forcings; of particular interest is when f is a parametric perturbation, e.g., $f(x,t) = A\cos(\omega t + \theta)x$, where parameters A, ω, θ represent the amplitude, frequency, and phase of the forcing, respectively.

[2]We also note overdamped Langevin (without timedependence) is a reversible Markov process, while kinetic Langevin considered here is irreversible, and its rare event quantification, even without the time-dependent perturbation, can be much more challenging; see, e.g., [56, 25, 60, 54, 35, 22, 23, 19, 12, 11, 50, 48, 59, 7, 34, 33]).

We will show explicitly that a specific choice of ω will lead to a parametric resonant enhancement of the transition rate. We remark that the terminology "resonance" here means that the quasi-potential/transition rate peaks at specific perturbation frequencies [17, 47], which is different from stochastic resonance [36] whereby the noise can lead to the amplification of the input signal.

To accomplish these goals, our point of departure is a higher-order Euler–Lagrange equation [44] characterization of the MLPs associated with second-order SDEs (which can be converted to a first-order system, however, with degenerate noise). Then we utilize a linear-theory calculation inspired by [17, 37, 2, 47] to approximate the minimum of Freidlin–Wentzell action (1.3) to the first order of ε. Specifically, our main contributions are (i) to develop a higher-order Hamiltonian formalism to reformulate time-dependent Freidlin–Wentzell action; (ii) to approximate the hopping rate between metastable periodic orbits of system (1.1) in terms of the unperturbed MLP explicitly, based on heteroclinic perturbation analysis; and (iii) to explicitly identify parametric resonant frequency in the context of metastable transition and uncover the impact of such resonance to the metastable transition rate in systems of practical relevance.

Several facts have to be mentioned: (i) To quantify the effect of external forcing on transition rate, we need to understand how MLPs in (1.1) change under the perturbation. After casting the rare event problem in second-order systems as a Hamiltonian formalism (for this formalism for first-order systems, see, e.g., [25, 30, 23, 9]), we will convert the transition rate quantification problem to the persistence of heteroclinic connections between periodic orbits after a nonautonomous Hamiltonian perturbation (similar problems have been considered in [18, 2], however, only for 1 degree of freedom (DOF)). Such persistence is a classical question in dynamical systems and has been answered by Melnikov [40, 24] for 1 DOF. One key issue with kinetic Langevin systems considered here is that Melnikov's approach is no longer directly applicable even in the single particle situation because it corresponds to a Hamiltonian system with 4 variables (2 DOF). Unfortunately, Melnikov's method was devised initially to compute the distance between stable and unstable manifolds only for planar Hamiltonian vector fields. Nevertheless, the perturbed heteroclinic connection as intersections of stable/unstable manifolds [58] can still be investigated. An inspiring article [8], for instance, extends Melnikov's method to give a condition under which the stable/unstable manifolds intersect transversely in a multidimensional setting. In essence, our approach is related to Melnikov's method but at the same time a generalization as we worked out the first-order perturbative expansion in higher dimensions. (ii) Unlike in the autonomous kinetic Langevin case considered in [48], one can no longer relate the perturbed MLPs to a second-order deterministic equation due to the loss of delicate statistical mechanical structure (which is, roughly speaking, a transverse decomposition [5] and consequent detailed balance after momentum reversible); instead, the forth-order Euler–Lagrange equation is necessary. To analyze it, we adopt a perturbation analysis for approximating the rate change along perturbed MLPs directly, which is independent of the specific form of perturbed MLPs. (iii) There have been previous studies on linear resonance, but our investigation in parametric resonance is, to the best of our knowledge, new.

The paper is organized as follows. Our general theory is in section 2. After reformulating the variational problem as a higher-order Hamiltonian formalism in subsection 2.1, we obtain an equivalent description of Freidlin–Wentzell action in subsection 2.2 and further characterize the transition rate in subsection 2.3. We then discuss the characterization of resonant frequency for parametric resonance in

section 3. Numerical experiments of parametric resonance are in section 4, and conclusions follow in section 5.

2. General theory. To simplify the notation, throughout the paper, we use symbols without superscript ε to represent quantities in the case of the unperturbed system, i.e., $\varepsilon = 0$.

2.1. Higher-order Lagrange and Hamiltonian formulation. To better understand the minimizer $x(t)$ (i.e., MLP) of Freidlin–Wentzell action functional $S^\varepsilon[x(t)]$, we start with the Euler–Lagrange equation of the higher-order variational principle [44], given by

$$\frac{\delta S^\varepsilon[x]}{\delta x} = \frac{\partial \mathcal{L}}{\partial x} - \frac{d}{dt}\frac{\partial \mathcal{L}}{\partial \dot{x}} + \frac{d^2}{dt^2}\frac{\partial \mathcal{L}}{\partial \ddot{x}} = 0, \tag{2.1}$$

equipped with boundary conditions $\lim_{t\to-\infty} x(t) - x_a^\varepsilon(t) = 0$, $\lim_{t\to+\infty} x(t) - x_b^\varepsilon(t) = 0$, where the Lagrangian $\mathcal{L}(t; x, \dot{x}, \ddot{x})$ is given by

$$\mathcal{L}(t; x, \dot{x}, \ddot{x}) = \frac{1}{2}\|\ddot{x} + \Gamma\dot{x} + \nabla V(x) - \varepsilon f(x,t)\|^2_{\Gamma^{-1}}. \tag{2.2}$$

Note that this differs from traditional Lagrangian mechanics, where $\mathcal{L}$ depends only on t, x, and $\dot{x}$, and the root of this difference lies in that noise is degenerate if we rewrite the kinetic Langevin equation as a first-order system. Consequently, the Euler–Lagrange equation (2.1) is a system of fourth-order differential equations for variable $x(t)$. Another remark is that, although each MLP solves the Euler–Lagrange equation, its solutions are not unique; later on we will establish a family of approximate solutions indexed by a parameter t_0.

We now convert this high-order Lagrangian problem to the Hamiltonian picture. For this purpose, let $q_1 = x$, $q_2 = \dot{x}$, and introduce new variables p_1, p_2 via

$$p_1 = \frac{\partial \mathcal{L}}{\partial \dot{x}} - \frac{d}{dt}\frac{\partial \mathcal{L}}{\partial \ddot{x}}, \quad p_2 = \frac{\partial \mathcal{L}}{\partial \ddot{x}}, \tag{2.3}$$

respectively, which are called generalized momentum of the prescribed system [44]. Then x solves Euler–Lagrange equations (2.1) if and only if

$$\dot{p}_1 = \frac{dp_1}{dt} = \frac{d}{dt}\frac{\partial \mathcal{L}}{\partial \dot{x}} - \frac{d^2}{dt^2}\frac{\partial \mathcal{L}}{\partial \ddot{x}} = \frac{\partial \mathcal{L}}{\partial x} = \frac{\partial \mathcal{L}}{\partial q_1}. \tag{2.4}$$

Since our Lagrangian $\mathcal{L}(t; x, \dot{x}, \ddot{x})$ satisfies the following nondegeneracy condition $\det(\frac{\partial^2 \mathcal{L}}{\partial \ddot{x} \partial \ddot{x}})_{nd\times nd} \neq 0$, it follows from the implicit function theorem that $\ddot{x}$ could be locally expressed as a function of t, q_1, q_2, p_2; denote it by

$$\ddot{x} = \mathbf{G}(t; q_1, q_2, p_2).$$

Define the Hamiltonian

$$\begin{aligned} H :&= H(t, q_1, q_2, p_1, p_2) = p_1 \cdot \dot{x} + p_2 \cdot \ddot{x} - \mathcal{L}(t; x, \dot{x}, \ddot{x}) \\ &= p_1 \cdot \dot{q}_1 + p_2 \cdot \mathbf{G}(t; q_1, q_2, p_2) - \mathcal{L}(t; q_1, q_2, \mathbf{G}(t; q_1, q_2, p_2)), \end{aligned}$$

where " $\cdot$ " represents the scalar product of vectors. It follows that

$$\begin{aligned}
&\frac{\partial H}{\partial q_1} = (D_{q_1}\mathbf{G}(t;q_1,q_2,p_2))^T p_2 - \frac{\partial \mathcal{L}}{\partial q_1} - (D_{q_1}\mathbf{G}(t;q_1,q_2,p_2))^T \frac{\partial \mathcal{L}}{\partial \ddot{x}} = -\frac{\partial \mathcal{L}}{\partial q_1},\\
&\frac{\partial H}{\partial q_2} = p_1 + (D_{q_2}\mathbf{G}(t;q_1,q_2,p_2))^T p_2 - \frac{\partial \mathcal{L}}{\partial q_2} - (D_{q_2}\mathbf{G}(t;q_1,q_2,p_2))^T \frac{\partial \mathcal{L}}{\partial \ddot{x}} = p_1 - \frac{\partial \mathcal{L}}{\partial q_2},\\
&\frac{\partial H}{\partial p_1} = \dot{q}_1,\\
&\frac{\partial H}{\partial p_2} = \mathbf{G}(t;q_1,q_2,p_2),
\end{aligned}$$

where $D_{q_1}\mathbf{G}$ (resp., $D_{q_2}\mathbf{G}$) denotes the gradient matrix of $\mathbf{G}$ with respect to variable q_1 (resp., q_2), and superscript "T" refers to transposition. Hence, the Euler–Lagrange equation (2.1) transform into the Hamiltonian differential equations

$$\dot{q_1} = \frac{\partial H}{\partial p_1}, \quad \dot{q_2} = \frac{\partial H}{\partial p_2}, \quad \dot{p_1} = -\frac{\partial H}{\partial q_1}, \quad \dot{p_2} = -\frac{\partial H}{\partial q_2}, \tag{2.5}$$

where we use (2.4) and the fact that $\dot{p}_2 = p_1 - \frac{\partial \mathcal{L}}{\partial \dot{x}}$ by (2.3). In fact, the above process can be reversed under the condition $\det(\frac{\partial^2 H}{\partial p_2 \partial p_2})_{nd\times nd} \neq 0$.

For the specific Lagrangian in (2.2), simplifications can be made, and the corresponding Euler–Lagrange equation is written in the equivalent Hamiltonian form

$$\begin{aligned}
&\dot{q}_1 = q_2, \qquad\qquad \dot{q}_2 = \Gamma p_2 - \Gamma q_2 - \nabla V(q_1) + \varepsilon f(q_1,t),\\
&\dot{p}_1 = (D_{q_1}\nabla V(q_1))^T p_2 - \varepsilon (D_{q_1} f(q_1,t))^T p_2, \quad \dot{p}_2 = \Gamma p_2 - p_1,
\end{aligned} \tag{2.6}$$

with Hamiltonian function

$$\begin{aligned}
H^\varepsilon(t,q_1,q_2,p_1,p_2) =& p_1^T \dot{q}_1 + p_2^T \dot{q}_2 - \frac{1}{2}\|\dot{q}_2 + \Gamma \dot{q}_1 + \nabla V(q_1) - \varepsilon f(q_1,t)\|^2_{\Gamma^{-1}}\\
=& p_1^T q_2 + p_2^T[\Gamma p_2 - \Gamma \dot{q}_1 - \nabla V(q_1) + \epsilon f(q_1,t)] - \frac{1}{2} p_2^T \Gamma p_2\\
=& \frac{1}{2} p_2^T \Gamma p_2 + p_1^T q_2 - p_2^T[\Gamma q_2 + \nabla V(q_1)] + \varepsilon p_2^T f(q_1,t) \qquad (2.7)\\
:=& H_0(q_1,q_2,p_1,p_2) + \varepsilon H_1(t,q_1,q_2,p_1,p_2). \qquad (2.8)
\end{aligned}$$

Therefore, each MLP in (1.1) corresponds to a solution of Hamilton's equations (2.6) (subject to boundary conditions). When $\varepsilon = 0$, the Hamiltonian system admits at least three hyperbolic fixed points $A(q_1 = x_a, q_2 = p_1 = p_2 = 0)$, $B(q_1 = x_b, q_2 = p_1 = p_2 = 0)$, and $O(q_1 = x_u, q_2 = p_1 = p_2 = 0)$ of the phase space (q_1,q_2,p_1,p_2), originated from the stable fixed points $(x_a,0)$, $(x_b,0)$ and saddle point $(x_u,0)$ of (1.1), respectively. Based on this higher-order Hamiltonian formalism, we now investigate how MLPs in (1.1) change under perturbation via understanding how heteroclinic connections in (2.6) change under perturbation.

Let us first consider the system (1.1) in the absence of perturbation, i.e., with $\varepsilon = 0$. It is known that MLPs among two local minima x_a, x_b of $V(x)$ correspond to the concatenation between the uphill heteroclinic orbits parametrized by $x_h^{(1)}(t)$ and downhill heteroclinic orbits $x_h^{(2)}(t)$ (e.g., [20, 48]) as long as they exist, which are described by

$$\ddot{x}_h^{(1)} - \Gamma \dot{x}_h^{(1)} + \nabla V(x_h^{(1)}) = 0, \quad x_h^{(1)}(-\infty) = x_a, \ \ x_h^{(1)}(+\infty) = x_u, \tag{2.9}$$

$$\ddot{x}_h^{(2)} + \Gamma \dot{x}_h^{(2)} + \nabla V(x_h^{(2)}) = 0, \quad x_h^{(2)}(-\infty) = x_u, \ \ x_h^{(2)}(+\infty) = x_b, \tag{2.10}$$

respectively, where x_u is a saddle of $V(x)$ and it serves as the transition from "uphill" to "downhill." The uphill (resp., downhill) heteroclinic orbit will be assumed to exist in this paper (the nonexistence is considered in [48] and not our focus).

To prepare for later treatments where ε is no longer zero, we note that $x_h^{(1)}(t-t_0)$ and $x_h^{(2)}(t-t_1)$ are also uphill and downhill heteroclinic orbits for any fixed phase parameter t_0 and t_1, respectively. A direct calculation shows they also satisfy (2.1) or (2.6) in the case of $\varepsilon = 0$, and thus we have the correspondence in (2.6), i.e.,

$$\begin{aligned} &q_{1,h}^{(1)}(t-t_0) = x_h^{(1)}(t-t_0), \qquad q_{2,h}^{(1)}(t-t_0) = \dot{x}_h^{(1)}(t-t_0), \\ &p_{2,h}^{(1)}(t-t_0) = 2q_{2,h}^{(1)}(t-t_0), \quad \dot{p}_{1,h}^{(1)} = \left(D_{q_{1,h}^{(1)}} \nabla V\left(q_{1,h}^{(1)}\right)\right)^T p_{2,h}^{(1)} \end{aligned} \tag{2.11}$$

and

$$\begin{aligned} &q_{1,h}^{(2)}(t-t_1) = x_h^{(2)}(t-t_1), \qquad q_{2,h}^{(2)}(t-t_1) = \dot{x}_h^{(2)}(t-t_1), \\ &p_{2,h}^{(2)}(t-t_1) = 0, \qquad\qquad\qquad \dot{p}_{1,h}^{(2)}(t-t_1) = 0, \end{aligned} \tag{2.12}$$

respectively. Indeed, these action-minimizing trajectories (2.11) (resp., (2.12)) are heteroclinic connections among two hyperbolic fixed points A (resp., O) and O (resp., B) of the forceless ($\varepsilon = 0$) Hamiltonian system (2.6). Note that the motion from A (resp., O) to O (resp., B) is the intersection of the unstable manifold of A (resp., O) and the stable manifold of O (resp., B) in their respective systems.

Now we return to the nonautonomously perturbed Hamiltonian system, i.e., (2.6) with $\varepsilon \neq 0$. Equivalently, we have the suspended system:

$$\begin{aligned} &\dot{\theta} = 1, \quad \dot{q}_1 = q_2, \quad \dot{q}_2 = \Gamma p_2 - \Gamma q_2 - \nabla V(q_1) + \varepsilon f(q_1, \theta), \\ &\dot{p}_1 = (D_{q_1} \nabla V(q_1))^T p_2 - \varepsilon (D_{q_1} f(q_1, t))^T p_2, \quad \dot{p}_2 = \Gamma p_2 - p_1, \end{aligned} \tag{2.13}$$

where $(q_1, q_2, p_1, p_2, \theta) \in \mathbb{R}^{4nd} \times \mathcal{S}^1$ ($\mathcal{S}^1 = \mathbb{R}/\tau_f$). For ε sufficiently small, (2.13) possesses a Poincaré map $\mathcal{P}_\varepsilon^{t_0} : \sum_{t_0} \to \sum_{t_0}$, where $\sum_{t_0} = \{(q_1, q_2, p_1, p_2, \theta) | \theta = t_0 \in [0, \tau_f]\} \subset \mathbb{R}^{4nd} \times \mathcal{S}^1$ is the global cross section[3] at time t_0 of the suspended autonomous flow. In the perturbed system (2.13) $\gamma_a = A \times \mathcal{S}^1$, $\gamma_b = B \times \mathcal{S}^1$, and $\gamma_u = O \times \mathcal{S}^1$, as periodic orbits of suspended system with $\varepsilon = 0$, are also perturbed. We will denote the perturbed (unique) periodic orbits by γ_a^ε, γ_b^ε, and γ_u^ε, respectively, the first component (q_1 component) of which gives periodic orbits $x_a^\varepsilon(t)$, $x_b^\varepsilon(t)$, $x_u^\varepsilon(t)$ of noiseless system (1.1). For generic Hamiltonians, the existence of the perturbed periodic orbits is guaranteed by implicit function theorem, at least for sufficiently small ε. We further assume that the heteroclinic trajectory connecting the unstable manifold of γ_a^ε (resp., γ_u^ε) and the stable manifold of γ_u^ε (resp., γ_b^ε) based on $\sum_{t_0}$ (resp., $\sum_{t_1}$) in system (2.6) survives after the nonautonomous forcing is switched on (i.e., $\varepsilon \neq 0$) (see Remark 2.1 for more details). Let us denote the perturbed instanton connection by the pair $q_{1,h}^{(i),\varepsilon}(t; t_{i-1}), q_{2,h}^{(i),\varepsilon}(t; t_{i-1}), p_{1,h}^{(i),\varepsilon}(t; t_{i-1}), p_{2,h}^{(i),\varepsilon}(t; t_{i-1})$, $i = 1, 2$. Then, by the equivalence of Hamiltonian (2.6) and Largangian mechanics (2.1), we also obtain the existence of heteroclinic connection $x_h^{(1),\varepsilon}(t; t_0)$ from $x_a^\varepsilon(t)$ to $x_u^\varepsilon(t)$ and heteroclinic orbit $x_h^{(2),\varepsilon}(t; t_1)$ from $x_u^\varepsilon(t)$ to $x_b^\varepsilon(t)$ in (2.1). Note that the initial times, t_0 and t_1, appear explicitly since solutions of the (2.1) are not invariant under arbitrary translations in time ((2.1) is nonautonomous for $\varepsilon \neq 0$).

[3] If the orbit of every point $(q_1, q_2, p_1, p_2, t) \in \mathbb{R}^{4nd+1}$ eventually crosses a $4nd$-dimensional surface $\sum_{t_0}$ and then returns to $\sum_{t_0}$ at a later time, then $\sum_{t_0}$ is a global section [39].

If $\varepsilon = 0$, the heteroclinic connections $x_h^{(1),\varepsilon}(t;t_0)$, $x_h^{(2),\varepsilon}(t;t_1)$ degenerate to the uphill and downhill heteroclinic orbits $x_h^{(1)}(t-t_0)$, $x_h^{(2)}(t-t_1)$, respectively. Different from the autonomous case described above (where the unperturbed action is invariant to the specific choice of t_0, t_1, e.g., [50, 48]), different t_0, t_1 give different local minima as the concatenation of $x_h^{(1),\varepsilon}(t;t_0)$ and $x_h^{(2),\varepsilon}(t;t_1)$ (for each fixed t_0, t_1 value) gives a critical point of the action for system (1.1).The reason for this difference lies in that the energy in (2.6) is not conserved and the action along the perturbed instanton now includes an integral of H^ε over time (see subsection 2.2 for the equivalence of the Fredlin–Wentzell action functional and the Hamiltonian action). Consequently, we optimize over t_0 and t_1 to obtain an MLP and the optimal transition rate of system (1.1). Thus (1.3) can be formally rewritten as follows [51]:

$$S^\varepsilon = \min_{t_0}\{S^\varepsilon[x_h^{(1),\varepsilon}(t;t_0)]\} + \min_{t_1}\{S^\varepsilon[x_h^{(2),\varepsilon}(t;t_1)]\}. \tag{2.14}$$

To compute (2.14), we will focus on the calculation of $S^\varepsilon[x_h^{(1),\varepsilon}(t;t_0)]$ since $S^\varepsilon[x_h^{(2),\varepsilon}(t;t_1)]$ will be, to the first order of ε, 0. That is, $S^\varepsilon = \min_{t_0} S^\varepsilon[x_h^{(1),\varepsilon}(t;t_0)]$ to the first order of ε. This is because $x_h^{(2),\varepsilon}(t;t_1)$ is moving along the perturbed downhill heteroclinic orbit as we will show in subsection 2.3 (a similar result originated from autonomous kinetic Langevin has been verified in [48]). From a physical point of view, the reason for such a result is that $x_h^{(2),\varepsilon}(t;t_1)$ is a relaxation trajectory i.e., once the system has approached the vicinity of an unstable periodic state $x_u^\varepsilon(t)$, it will eventually be attracted to another stable periodic state $x_b^\varepsilon(t)$ with a probability $\sim 1/N$ (which goes into the prefactor; N is the number of attraction basins whose boundaries include x_u^ε), without requiring extra noise. Thus, in order to quantify the metastable transition rate between $x_a^\varepsilon(t)$ and $x_b^\varepsilon(t)$ in this case, we convert it to an escape problem from the vicinity of the stable periodic state $x_a^\varepsilon(t)$ to that of unstable one $x_u^\varepsilon(t)$.

Remark 2.1. The perturbed system (2.6) will not, in general, maintain the intersection between the unstable and stable manifolds of A (resp., O) and O (resp., B) [18]: these manifolds might intersect, preserving the existence of the heteroclinic connection, but they also might not, in which case the heteroclinic connection is destroyed. Interestingly, Capinski and Zgliczynski [8] proposed a Melnikov-type approach for establishing transversal intersections of stable/unstable manifolds in a multidimensional setting. This result could ensure the existence of heteroclinic connections in system (2.6) if appropriate conditions are imposed. Nevertheless, for simplicity we just assume ε is small enough so that a heteroclinic connection in the perturbed system exists.

2.2. Reformulation of the Fredlin–Wentzell action functional. As described above, to obtain the minimum of the Freidlin–Wentzell action functional, the core of this calculation is the transition from the stable periodic orbit $x_a^\varepsilon(t)$ to the unstable one $x_u^\varepsilon(t)$. And our strategy will be to calculate the action along the perturbed instanton, which is the heteroclinic connection of the perturbed, time-dependent Hamiltonian system (2.6). More concretely, we start by reformulating the action functional $S^\varepsilon[\cdot]$ in (1.3) in a form convenient in this subsection and then conduct a derivation on correction of the action in subsequent subsection 2.3. For simplicity of exposition, we drop the superscript "(1)" in notation $x_h^{(1)}(t)$, $x_h^{(1).\varepsilon}(t;t_0)$.

Let us now consider a Hamiltonian action

$$\begin{aligned} A^\varepsilon[\gamma] &= \int_\gamma p_1^T dq_1 + p_2^T dq_2 - H^\varepsilon dt \\ &= \int_{-\infty}^{\infty} p_1^T(t)\frac{dq_1}{dt} + p_2^T(t)\frac{dq_2}{dt} - H^\varepsilon(t, q_1(t), q_2(t), p_1(t), p_2(t))dt, \end{aligned} \tag{2.15}$$

where γ is a path in phase space. To be more precise, $\gamma : (-\infty, \infty) \to \mathbb{R}^{4nd}$ and is denoted by $\gamma = \{(q_1^T(t), q_2^T(t), p_1^T(t), p_2^T(t)), -\infty < t < \infty\}$. H^ε takes the form of (2.7). We remark that variables q_1, q_2, p_1, p_2 in (2.15) are mutually independent. It is well known (e.g., [39]) that the curve of stationary action (2.15) is the Hamiltonian trajectory (2.6). We further have the following result.

PROPOSITION 2.2. *$S^\varepsilon[x] = A^\varepsilon[\gamma]$ along the instanton solutions of* (2.1) *or* (2.6). *That is,*

$$S^\varepsilon\left[x_h^\varepsilon(t;t_0)\right] = A^\varepsilon\left[\left(q_{1,h}^\varepsilon(t;t_0), q_{2,h}^\varepsilon(t;t_0), p_{1,h}^\varepsilon(t;t_0), p_{2,h}^\varepsilon(t;t_0)\right)\right], \tag{2.16}$$

which is dependent of t_0 with $t_0 \in [0, \tau_f]$ when $\varepsilon \neq 0$. Here $x_h^\varepsilon(t;t_0) = q_{1,h}^\varepsilon(t;t_0)$ is a heteroclinic connection connecting $x_a^\varepsilon(t)$ and $x_u^\varepsilon(t)$ in system (2.1), *and a relation between $x_h^\varepsilon(t;t_0)$ and $q_{2,h}^\varepsilon(t;t_0)$, $p_{1,h}^\varepsilon(t;t_0)$, $p_{2,h}^\varepsilon(t;t_0)$ is given by* (2.3).

Proposition 2.2 holds as a result of the equivalence of Hamiltonian and Lagrangian mechanics under the Legendre condition. For more details on the proof of Proposition 2.2, the reader is referred to [39].

To prepare for the next subsection, we further calculate the minimum of the Freidlin–Wentzell action functional for system (1.1) in the absence of ε. In view of (2.15), (2.7), (2.9), we get

$$\begin{aligned} A_0 &= \int_{-\infty}^{\infty}[p_{1,h}^T\dot{q}_{1,h} + p_{2,h}^T\dot{q}_{2,h} - H_0(q_{1,h}, q_{2,h}, p_{1,h}, p_{2,h})]dt \\ &= \int_{-\infty}^{\infty} p_{1,h}^T q_{2,h} + 2q_{2,h}^T\dot{q}_{2,h} - p_{1,h}^T q_{2,h} + 2\dot{q}_{1,h}^T\nabla V(q_{1,h})dt \\ &= 2[V(x_u) - V(x_a)], \end{aligned}$$

$$\begin{aligned} S_0 = S[x_h] &= \tfrac{1}{2}\int_{-\infty}^{\infty} \|\ddot{x}_h + \Gamma\dot{x}_h + \nabla V(x_h)\|_{\Gamma^{-1}}^2 dt \\ &= \tfrac{1}{2}\int_{-\infty}^{\infty} \|\ddot{x}_h - \Gamma\dot{x}_h + \nabla V(x_h)\|_{\Gamma^{-1}}^2 + 4\dot{x}_h^T(\ddot{x}_h + \nabla V(x_h))dt \\ &= 2[V(x_u) - V(x_a)] \end{aligned}$$

if we choose homogeneous velocity boundary conditions $\dot{x}_h(+\infty) = 0$, $\dot{x}_h(-\infty) = 0$, where $x_h(t)$ is an uphill heteroclinic orbit given in (2.9). Again we get $S_0 = A_0$.

Remark 2.3. Proposition 2.2 also holds for the case of x_u^ε(t) to $x_b^\varepsilon(t)$ transition, with the corresponding value of action S_0 being 0 [48] when $\varepsilon = 0$ (because downhill heteroclinic orbit $x_h^{(2)}(t)$ by definition (2.10) is the zero of $\frac{1}{2}\int_{-\infty}^{+\infty} \|\ddot{x} + \Gamma\dot{x} + \nabla V(x)\|_{\Gamma^{-1}}^2 dt$).

2.3. Relating the minimizers of $S^\varepsilon[\cdot]$ and $S[\cdot]$. In the following, we will use the reformulation (2.16) to study the relationship between $S^\varepsilon[\cdot]$ and $S[\cdot]$. To do so, it is equivalent to deal with the relationship between $A^\varepsilon[\cdot]$ and $A[\cdot]$.

In light of Proposition 2.2, we provide a linear-theory calculation of the action $S^\varepsilon[\cdot]$ inspired by [2] and approximate the rate of the metastable transition. Assume $\varepsilon \ll 1$ so that the term $H_1(t, q_1, q_2, p_1, p_2)$ in (2.7) can be treated perturbatively. Let us expand the perturbed instanton of $H^\varepsilon(t, q_{1,h}^\varepsilon(t;t_0), q_{2,h}^\varepsilon(t;t_0), p_{1,h}^\varepsilon(t;t_0), p_{2,h}^\varepsilon(t;t_0))$ to the first order in ε:

$$q_{1,h}^\varepsilon(t;t_0) = q_{1,h}(t-t_0) + \varepsilon Q_{1,h}(t;t_0) + \mathcal{O}(\varepsilon^2), \quad q_{2,h}^\varepsilon(t;t_0) = q_{2,h}(t-t_0) + \varepsilon Q_{2,h}(t;t_0) + \mathcal{O},$$
$$p_{1,h}^\varepsilon(t;t_0) = p_{1,h}(t-t_0) + \varepsilon P_{1,h}(t;t_0) + \mathcal{O}(\varepsilon^2), \quad p_{2,h}^\varepsilon(t;t_0) = p_{2,h}(t-t_0) + \varepsilon P_{2,h}(t;t_0) + \mathcal{O},$$

where $\mathcal{O} = \mathcal{O}(\varepsilon^2)$, $q_{1,h}(t-t_0) = x_h(t-t_0)$ satisfies uphill dynamics (2.9), and it's combined with $q_{2,h}(t-t_0)$, $p_{1,h}(t-t_0)$, $p_{2,h}(t-t_0)$ to stand for the (known) instanton solution of (2.6) with $\varepsilon = 0$. To calculate the action $A^\varepsilon[\cdot]$ given in (2.15), we expand the integrand in ε by a Taylor theorem and obtain, in the first order,

$$\begin{aligned}
&(p_{1,h}+\varepsilon P_{1,h})^T(\dot q_{1,h}+\varepsilon\dot Q_{1,h}) + (p_{2,h}+\varepsilon P_{2,h})^T(\dot q_{2,h}+\varepsilon\dot Q_{2,h})\\
&\quad - H_0(q_{1,h},q_{2,h},p_{1,h},p_{2,h}) - \varepsilon Q_{1,h}^T\frac{\partial H_0}{\partial q_{1,h}} - \varepsilon Q_{2,h}^T\frac{\partial H_0}{\partial q_{2,h}} - \varepsilon P_{1,h}^T\frac{\partial H_0}{\partial p_{1,h}} - \varepsilon P_{2,h}^T\frac{\partial H_0}{\partial p_{2,h}}\\
&\quad - \varepsilon H_1(q_{1,h},q_{2,h},p_{1,h},p_{2,h})\\
\simeq& p_{1,h}^T\dot q_{1,h} + p_{2,h}^T\dot q_{2,h} - H_0(q_{1,h},q_{2,h},p_{1,h},p_{2,h}) + \varepsilon p_{1,h}^T\dot Q_{1,h} + \varepsilon P_{1,h}^T\dot q_{1,h} + \varepsilon p_{2,h}^T\dot Q_{2,h}\\
&\quad + \varepsilon P_{2,h}^T\dot q_{2,h} + \varepsilon Q_{1,h}^T\dot p_{1,h} + \varepsilon Q_{2,h}^T\dot p_{2,h} - \varepsilon P_{1,h}^T\dot q_{1,h} - \varepsilon P_{2,h}^T\dot q_{2,h}\\
&\quad - \varepsilon H_1(q_{1,h},q_{2,h},p_{1,h},p_{2,h})\\
=& p_{1,h}^T\dot q_{1,h} + p_{2,h}^T\dot q_{2,h} - H_0(q_{1,h},q_{2,h},p_{1,h},p_{2,h}) + \varepsilon p_{1,h}^T\dot Q_{1,h} + \varepsilon Q_{1,h}^T\dot p_{1,h} + \varepsilon p_{2,h}^T\dot Q_{2,h}\\
&\quad + \varepsilon Q_{2,h}^T\dot p_{2,h} - \varepsilon H_1(q_{1,h},q_{2,h},p_{1,h},p_{2,h}).
\end{aligned}$$

After the integration, the first three terms yield the unperturbed action S_0. The fourth and fifth terms give the time derivative of $\varepsilon p_{1,h}^T Q_{1,h}$, and the sixth and seventh terms give the time derivative of $\varepsilon p_{2,h}^T Q_{2,h}$. Taking the boundary conditions into account, these four terms vanish after integration. Therefore, there is no contribution from the perturbations $Q_{i,h}$, $P_{i,h}$, $i = 1, 2$ at the $\mathcal{O}(\varepsilon)$ order. Hence, the result is $S^\varepsilon(t_0) = S_0 + \varepsilon\delta S(t_0)$, where

$$\begin{aligned}
\delta S(t_0) &= -\int_{-\infty}^{+\infty} H_1\big(t, q_{1,h}(t-t_0), q_{2,h}(t-t_0), p_{1,h}(t-t_0), p_{2,h}(t-t_0)\big)dt\\
&= -\int_{-\infty}^{+\infty} p_{2,h}(t-t_0)^T f(q_{1,h}(t-t_0),t)dt \qquad (2.17)\\
&= -2\int_{-\infty}^{+\infty} \dot x_h^T(t-t_0) f(x_h(t-t_0),t)dt. \qquad (2.18)
\end{aligned}$$

The last step is based on relation (2.11). To find the optimal first-order correction to the minimum action's value, we have to minimize $S^\varepsilon(t_0)$ with respect to t_0, which thus yields the equation for optimal t_0:

$$\int_{-\infty}^{+\infty}\Big[\dot x_h^T(t-t_0)\nabla f(x_h(t-t_0),t)\dot x_h(t-t_0) + \ddot x_h^T(t-t_0) f(x_h(t-t_0),t)\Big]\,dt = 0.$$

We now summarize the above results in a concise form as follows

THEOREM 2.4. *Consider nonautonomous kinetic Langevin system* (1.1). *Assume that a heteroclinic connection from x_a to x_u exists in the noiseless ($\mu = 0$) and forceless ($\varepsilon = 0$) backward in time system, and ε is small enough such that a heteroclinic connection from $x_a^\varepsilon(t)$ to $x_u^\varepsilon(t)$ exists in Euler–Lagrange equation* (2.1). *Then the escape rate from stable periodic orbit $x_a^\varepsilon(t)$ to unstable (hyperbolic) periodic orbit $x_u^\varepsilon(t)$ is asymptotically equivalent to* $\exp(-S^\varepsilon/\mu)$, *where $S^\varepsilon = 2[V(x_u)-V(x_a)]+\varepsilon\delta S_e+\mathcal{O}(\varepsilon^2)$, and δS_e characterizes the leading-order effect of external driving on metastable transition. δS_e is given by*

$$\delta S_e = \min_{t_0}\delta S(t_0), \quad \delta S(t_0) = -2\int_{-\infty}^{+\infty}\dot x_h^T(t-t_0) f(x_h(t-t_0),t)dt, \qquad (2.19)$$

where $x_h(t)$ satisfies

$$\ddot{x}_h - \Gamma\dot{x}_h + \nabla V(x_h) = 0, \quad x_h(-\infty) = x_a, \ \ x_h(+\infty) = x_u. \tag{2.20}$$

Here, x_a, x_u are the local minimum and saddle point of potential $V(x)$, respectively.

Remark 2.5. Theorem 2.4 is consistent with the results of [17] which considered the $n = d = 1$, $\Gamma = \gamma$, and $f(x,t) = f(t)$ case. Different from [17], our method is also applicable to high-dimensional Langevin systems with general (time-dependent, nonlinear) perturbation, while [17] focused on 1-dimensional Langevin equations with additive periodic perturbation based on the idea of path integral.

Remark 2.6. For the general case where Γ depends on position and velocity, i.e., $\Gamma(x,\dot{x})$, Theorem 2.4 still holds with slight modification, i.e., replacing Γ by $\Gamma(x,\dot{x})$.

A similar procedure can be used to understand the $x_u^\varepsilon(t)$ to $x_b^\varepsilon(t)$ transition, and $\delta S(t_0)$ given in (2.17) will vanish in this case due to (2.12). Together with Remark 2.3, we verify that $S^\varepsilon[x_h^{(2),\varepsilon}(t;t_1)]$ in (2.14) is zero to the first order of ε. Consequently, combining with Theorem 2.4, a natural result on metastable transition rate is the following.

THEOREM 2.7. *Under the same conditions as stated in Theorem* 2.4*, further assume that x_u is the only attractor on the separatrix between the basins of attraction of x_a and x_b, a heteroclinic connection from x_u to x_b exists in the noiseless ($\mu = 0$) and forceless ($\varepsilon = 0$) system, and ε is small enough such that a heteroclinic connection from $x_u^\varepsilon(t)$ to $x_b^\varepsilon(t)$ exists in Euler–Lagrange equation* (2.1)*. Then the transition rate from stable periodic orbit $x_a^\varepsilon(t)$ to another stable periodic orbit $x_b^\varepsilon(t)$ is asymptotically equivalent to $\exp(-S^\varepsilon/\mu)$, where $S^\varepsilon = 2[V(x_u) - V(x_a)] + \varepsilon\delta S_e + \mathcal{O}(\varepsilon^2)$, and δS_e is described in Theorem* 2.4*.*

Example 2.8. Let us consider two special forms of forcing $f(x,t)$, the first being the linear forcing already considered in the literature and the second being a parametric forcing (see, e.g., [41, 31, 52, 49, 57] for existing applications to deterministic systems). They will be used later to demonstrate the resonant enhancement of the transition rate. For a simple illustration, each component of $f(x,t)$ is chosen to be of the same type (although one can treat arbitrary components of general forcing $f(x,t)$ simply by substituting it into the expression (2.19) in Theorem 2.4 and calculate integral $\delta S(t_0)$ in (2.19)).

(i) For a sinusoidal field $(f(t))_j = A_j\cos(\omega_j t + \theta_j), j = 1,\dots,nd$, where parameters A_j, ω_j, θ_j represent the amplitude, frequency, and phase of jth component of forcing, respectively, the correction δS_e becomes

$$\delta S_e = \min_{t_0}\delta S(t_0) = \min_{t_0}\left\{-2\sum_{j=1}^{nd}\cos(\omega_j t_0 + \theta_j + \phi_j)\Big|\int_{-\infty}^{\infty} A_j\dot{x}_h^j(t)e^{i\omega_j t}dt\Big|\right\}.$$

Here, $\dot{x}_h^j(t)$ denotes the jth component of $x_h(t)$ the calculation of $\delta S(t_0)$ is as follows:

$$\begin{aligned}
\delta S(t_0) &= -2\int_{-\infty}^{+\infty}\left[\sum_{j=1}^{nd} A_j\dot{x}_h^j(t)\cos(\omega_j(t+t_0)+\theta_j)\right]dt \\
&= -\sum_{j=1}^{nd}\left\{e^{i(\omega_j t_0+\theta_j)}\int_{-\infty}^{+\infty} A_j\dot{x}_h^j(t)e^{i\omega_j t}dt + e^{-i(\omega_j t_0+\theta_j)}\int_{-\infty}^{+\infty} A_j\dot{x}_h^j(t)e^{-i\omega_j t}dt\right\} \\
&= -2\sum_{j=1}^{nd}\left[\cos(\omega_j t_0+\theta_j)\Re\left(\int_{-\infty}^{+\infty} A_j\dot{x}_h^j(t)e^{i\omega_j t}dt\right)\right.
\end{aligned}$$

$$- \sin(\omega_j t_0 + \theta_j)\Im\left(A_j \int_{-\infty}^{+\infty} \dot{x}_h^j(t) e^{i\omega_j t} dt\right)\Big]$$
$$= -2\sum_{j=1}^{nd} \cos(\omega_j t_0 + \theta_j + \phi_j)\left|A_j \int_{-\infty}^{\infty} \dot{x}_h^j(t) e^{i\omega_j t} dt\right|,$$

where $\sin\phi_j = \frac{\Im(\int_{-\infty}^{\infty} \dot{x}_h^j(t) e^{i\omega_j t} dt)}{|\int_{-\infty}^{\infty} \dot{x}_h^j(t) e^{i\omega_j t} dt|}$. Note that, for a special homogeneous case where $\omega_j = \omega$, $\theta_j = \theta$ for $j = 1, \ldots, nd$, the optimal t_0 can be determined explicitly, and thus simplification occurs. Specifically, $\delta S_e = -2|\sum_{j=1}^{nd} A_j \int_{-\infty}^{\infty} \dot{x}_h^j(t) e^{i\omega t} dt|$. This is because

$$\begin{aligned}
\delta S(t_0) =& -2\int_{-\infty}^{+\infty} \left[\sum_{j=1}^{nd} A_j \dot{x}_h^j(t)\right] \cos(\omega(t + t_0) + \theta) dt \\
=& -\left[e^{i(\omega t_0 + \theta)} \int_{-\infty}^{+\infty} \sum_{j=1}^{nd} A_j \dot{x}_h^j(t) e^{i\omega t} dt + e^{-i(\omega t_0 + \theta)} \int_{-\infty}^{+\infty} \sum_{j=1}^{nd} A_j \dot{x}_h^j(t) e^{-i\omega t} dt\right] \\
=& -2\cos(\omega t_0 + \theta + \phi)\left|\sum_{j=1}^{nd} A_j \int_{-\infty}^{\infty} \dot{x}_h^j(t) e^{i\omega t} dt\right|,
\end{aligned}$$

where $\sin\phi = \frac{\Im(\sum_{j=1}^{nd} A_j \int_{-\infty}^{\infty} \dot{x}_h^j(t) e^{i\omega t} dt)}{|\sum_{j=1}^{nd} A_j \int_{-\infty}^{\infty} \dot{x}_h^j(t) e^{i\omega t} dt|}$. Thus $\delta S_e = -2|\sum_{j=1}^{nd} A_j \int_{-\infty}^{\infty} \dot{x}_h^j(t) e^{i\omega t} dt|$. We see that the initial phase θ doesn't affect δS_e.

(ii) For forcing in the form of $(f(x,t))_j = A_j \cos(\omega_j t + \theta_j) x_j, j = 1, \ldots, nd$, the correction δS_e takes the form of

$$\delta S_e = \min_{t_0} \delta S(t_0) = \min_{t_0} \left\{-2\sum_{j=1}^{nd} \cos(\omega_j t_0 + \theta_j + \phi_j)\left|\int_{-\infty}^{\infty} A_j \dot{x}_h^j(t) x_h^j(t) e^{i\omega_j t} dt\right|\right\},$$

where $\sin\phi_j = \frac{\Im(\int_{-\infty}^{\infty} \dot{x}_h^j(t) x_h^j(t) e^{i\omega_j t} dt)}{|\int_{-\infty}^{\infty} \dot{x}_h^j(t) x_h^j(t) e^{i\omega_j t} dt|}$. Again, δS_e takes a more simple form of $\delta S_e = -2|\sum_{j=1}^{nd} A_j \int_{-\infty}^{\infty} \dot{x}_h^j(t) x_h^j(t) e^{i\omega_j t} dt|$ when the homogeneous case where $\omega_j = \omega$, $\theta_j = \theta$ for $j = 1, \ldots, nd$ is considered, which can be derived by a similar arguments as case (i). Here, $\sin\phi = \frac{\Im(\sum_{j=1}^{nd} A_j \int_{-\infty}^{\infty} \dot{x}_h^j(t) x_h^j(t) e^{i\omega t} dt)}{|\sum_{j=1}^{nd} A_j \int_{-\infty}^{\infty} \dot{x}_h^j(t) x_h^j(t) e^{i\omega t} dt|}$.

In both cases, δS_e is dependent on the input frequency ω_j. In certain applications such as molecular systems, one may not have enough resolution to force each DOF at a different frequency, and we thus can consider for simplicity a special homogeneous case where $\omega_1 = \cdots = \omega_n = \omega$, $\theta_1 = \cdots = \theta_n = \theta$. Even in this case, there exist special values of ω that make the action δS_e vary greatly as we will show in section 3, and each such ω will be called a resonant frequency. Consistent with physical intuitions, resonant frequencies are related to the intrinsic frequencies of the unperturbed system (2.20). Thanks to Theorem 2.4, we will show that, if the heteroclinic connection of the unperturbed system (2.20) can be found, we can determine the resonant frequencies, without any rare event simulation which is computationally very costly, no matter how high-dimensional and how nonlinear the original system (1.1) is.

3. Parameteric resonance: Characterization of the resonant frequency. As the general effect of time-dependent forcing on metastable transition has been discussed in the previous section, we now move on to focus on specific forcings. One observation is that, when the forcing takes the form of $f(x,t) = A\cos(\omega t + \theta)x$, a resonance-like mechanism will prevail, namely, that there exists a special input frequency that leads to a significantly stronger reduction of quasi-potential (and

hence enhanced transition rate). This phenomenon is referred to as parametric resonance.[4]

We will use the stationary phase method to estimate the resonant frequency of parametric resonance based on Example 2.8. For the sake of simplicity, we will detail the method on single particle cases, i.e., $n = 1, d = 1, \Gamma = \gamma$. Then we will outline the idea of a generalization to higher dimensions in Remark 3.2.

The heteroclinic connection of the forceless deterministic system. To understand why there is a resonant frequency and what it is, we will utilize the assumption that the system is underdamped (i.e., γ small) and perform asymptotic estimations (approximation sign "$\approx$" in the following presentation means equal sign "$=$" in the $\gamma \to 0$ limit). More precisely, letting $q = x$, $p = \dot{x}$, Hamiltonian $H(q,p) = p^2/2 + V(q)$, and energy $E(t) = H(q(t), p(t))$, the forceless heteroclinic connection corresponds to fast oscillation along the Hamiltonian level set and slow change of the energy value (as the heteroclinic connection goes uphill). Following [17], we express the configuration and velocity variables of the heterclinic connection by

$$\begin{aligned} q(t) &= \sum_{n=-\infty}^{+\infty} q_n(E(t)) \exp(-in\varphi(t)), \qquad & \dot{E}(t) &\approx \gamma\omega(E)I(E), \\ p(t) = \dot{q}(t) &= \sum_{n=-\infty}^{+\infty} p_n(E(t)) \exp(-in\varphi(t)), \qquad & \dot{\varphi} &= \omega(E(t)), \end{aligned} \tag{3.1}$$

where I and φ are action and angle variables, $\omega(E(t))$ is the frequency of oscillation in Hamiltonian system H at energy $E(t)$, $q_n(E(t))$ and $p_n(E(t))$ are, respectively, the amplitude of the nth overtone of the configuration $q(t)$ and the momentum $p(t)$, and the last line of (3.1) is obtained via averaging $\dot{E} = \gamma p^2$ over the oscillations.

Parametric resonant frequency. For the case of parametric perturbation $f(q,t) = A\cos(\Omega t + \theta)q$, by applying Theorem 2.7 and Example 2.8, the change of transition rate is characterized by $\delta S_e = -2A|\int_{-\infty}^{\infty} \dot{q}_h(t) q_h(t) e^{i\Omega t} dt|$. For convenience, denote $|\int_{-\infty}^{\infty} \dot{q}_h(t) q_h(t) e^{i\Omega t} dt|$ by $|I(\Omega)|$. Substitution of (3.1) into this δS_e gives

$$\begin{aligned} I(\Omega) &= \int_{-\infty}^{+\infty} \left(\sum_{n=-\infty}^{+\infty} p_n[E(t)] e^{-in\varphi(t)} \right) \left(\sum_{m=-\infty}^{+\infty} q_m[E(t)] e^{-im\varphi(t)} \right) e^{i\Omega t} dt \\ &= \int_{-\infty}^{+\infty} \sum_{l=-\infty}^{+\infty} e^{-il\varphi(t)} \left(\sum_{m=-\infty}^{+\infty} p_{l-m}[E(t)] q_m[E(t)] \right) e^{i\Omega t} dt \\ &= \frac{1}{\gamma} \int_{-\infty}^{+\infty} \sum_{l=-\infty}^{+\infty} a_l[E(\tau)] \exp\left[i \frac{1}{\gamma} \big(\Omega\tau - l\psi(\tau) \big) \right] d\tau. \end{aligned} \tag{3.2}$$

Here we use a_l to denote $\sum_{m=-\infty}^{+\infty} p_{l-m}[E(t)] q_m[E(t)]$ for simplicity. Note that the last step in (3.2) is based on the change of variable $t = \frac{1}{\gamma}\tau$, because of which we further obtain that $\frac{d\varphi}{d\tau} = \frac{1}{\gamma}\omega(E)$, $\frac{dE}{d\tau} \approx \omega(E)I(E)$, and the function $\psi(\tau) = \gamma\varphi(\tau)$ satisfies $\frac{d\psi}{d\tau} = \omega(E)$.

For a smooth heteroclinic connection induced by smooth potential V, a_l decays exponentially, and the integral and infinite sum can be exchanged. We thus consider each term and denote it by

[4] We call it parametric resonance because the forcing is a parametric perturbation. If $f(x,t) = A\cos(\omega t + \theta)$ instead, a similar phenomenon will be called linear resonance.

$$I_l(\Omega) = \frac{1}{\gamma}\int_{-\infty}^{+\infty} a_l[E(\tau)] \exp\left[i\frac{1}{\gamma}\big(\Omega\tau - l\psi(\tau)\big)\right] d\tau. \tag{3.3}$$

Also because a_l typically decays very fast as $|l|$ increases, in the presentation below we focus on the Ω value that resonates with the dominating mode, denoted also by l under slightly abused notation (unless confusion arises, which will be clarified then). Usually the fundamental frequency is the dominating mode, i.e., $l = 1$. In less common cases when $a_1 = a_{-1} = 0$ (e.g., if $\ddot{q}_h + \omega^2(1 + \epsilon\cos(\Omega t))q_h = 0$, then this happens and the resonant frequency is actually $\Omega = 2\omega$ instead of $\Omega = \omega$, i.e., $l = 2$ instead; this toy q_h is not a heteroclinic connection though) or when multiple overtones have comparable amplitudes, there is one resonant frequency associated with each dominating mode.

Away from a stationary phase, the integrand in (3.3) has a slowly varying amplitude but a fast oscillating phase, and it thus mostly cancels out after the integration. If τ has a stationary phase, however, the integral will have a much larger value due to the contribution in the proximity of this stationary phase. This is the intuition behind the choice of a resonant Ω. More precisely, the phase becomes stationary when $\frac{d}{d\tau}\big(\Omega\tau - l\psi(\tau)\big) = 0$, i.e., $\Omega = l\omega(E(\tau^*))$, where τ^* is a stationary point of phase. This gives the value of resonant Ω. We now further understand its details.

To do so, we first define a notion of intrinsic frequency. Consider the uphill hetericlinic orbit equation:

$$\ddot{q}_h - \gamma\dot{q}_h + V'(q_h) = 0, \quad q_h(-\infty) = x_a, \ \ q_h(+\infty) = x_u. \tag{3.4}$$

By linearizing $V'(q)$ around $q = x_a$, we obtain

$$\ddot{q}_h - \gamma\dot{q}_h + V''(x_a)q_h = 0,$$

whose characteristic equation has eigenvalues $r = \frac{\gamma}{2} \pm i\sqrt{V''(x_a) - \frac{\gamma^2}{4}}$. Note that there are two eigenvalues as long as the imaginary part is nonzero (note γ is small), corresponding to the general solutions $q_h(t) \approx Me^{\frac{\gamma}{2}t}e^{i\sqrt{V''(x_a)-\frac{\gamma^2}{4}}} + Ne^{\frac{\gamma}{2}t}e^{-i\sqrt{V''(x_a)-\frac{\gamma^2}{4}}}$, in which M, N are arbitrary constants. These solutions in general describe oscillation at frequency $\omega = \sqrt{V''(x_a) - \frac{\gamma^2}{4}}$. We call $\omega_0 = \sqrt{V''(x_a)}$ the intrinsic frequency as we're using $\gamma \to 0$ asymptotics, although denoting the intrinsic frequency by $\omega_0 = \sqrt{V''(x_a) - \frac{\gamma^2}{4}}$ will not affect the results either.

In (3.4), the heteroclinic orbit $q_h(t)$ circles around the metastable state x_a (corresponding to minimal $E_m = V(x_a)$) with intrinsic frequency ω_0 for an infinite amount of time (see Figure 1(a) for an illustration). In this phase, the slowly changing energy $E(t)$ is $E(\tau^*) = E_m$ (for γ small enough). We thus obtain resonant frequency $\Omega = l\omega(E(\tau^*)) = l\omega_0$.

We then estimate $|I_1(\Omega)|$. Let $\bar{\psi}(\tau) = \Omega\tau - \psi(\tau)$ which has a stationary point at $\tau = \tau^*$ with

$$\bar{\psi}'(\tau^*) = 0, \bar{\psi}''(\tau^*) = -\frac{d\omega(E)}{dE}\frac{dE}{d\tau}\Big|_{\tau=\tau^*} \approx -\frac{d\omega(E)}{dE}I(E)\omega(E)\Big|_{\tau=\tau^*} \neq 0.$$

Evaluating the integral $I_1(\Omega)$ by the method of stationary phase (see, e.g., [53]), get

$$|I_1(\Omega)| \sim \left[\frac{1}{\sqrt{\gamma}}|a_1(E)|\sqrt{\frac{2\pi}{\left|\frac{d\omega(E)}{dE}I(E)\omega(E)\right|}}\right]_{\tau=\tau^*} \quad \text{in the small } \gamma \text{ regime.} \tag{3.5}$$

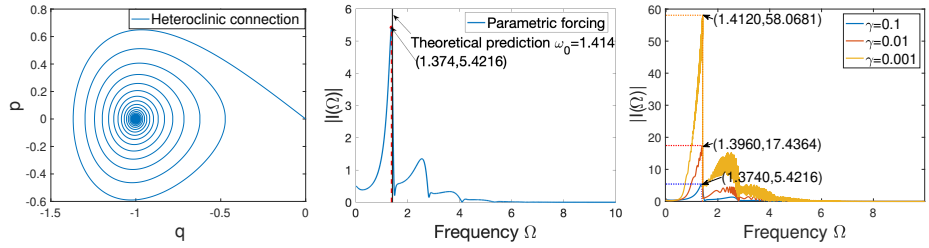

(a) (b) (c)

FIG. 1. *(Color online)* (a) *A heteroclinic connection (or MLP) from* -1 *to* 0 *in phase space:* $\gamma = 0.1$, $p = \dot{q}$ *denotes momentum of the particle.* (b) $\delta S = -2A\epsilon|I(\Omega)|$*: damping* $\gamma = 0.1$*. The dependence of action correction* $|I(\Omega)|$ *of the double-well system on frequency* Ω *in the case of parametric forcing. Black solid line: theoretically predicted resonance frequency* $\omega_0 = 1.414$*; red dot line: passing through the numerical observed peak* $(1.374, 5.4216)$. (c) $\delta S = -2A\epsilon|I(\Omega)|$*. The dependence of action correction* $|I(\Omega)|$ *of the stochastic double-well system on frequency* Ω *for different damping* $\gamma = 0.1, 0.01, 0.001$*, respectively.*

The symbol "$\sim$" means that the left- and right-hand sides agree at the leading order in an asymptotic expansion in γ. This quantitative result shows that, for example, a smaller friction coefficient corresponds to a bigger change of transition rate induced by the parametric excitation.

Remark 3.1. Similar to linear resonance already considered in literature (see, e.g., [17]), the parametric resonant frequency also corresponds to intrinsic frequency ω_0. This may sound inconsistent with the parametric resonant frequency of linear (e.g., $\ddot{q}_h + \omega_0^2(1 + \epsilon\cos(\Omega t))q_h = 0$) or weakly nonlinear systems (e.g., [49, 51]) which is $\Omega = 2\omega_0$, but the latter is in fact, as discussed above, a special case where $a_1 = a_{-1} = 0$. As the potential of our system is in general arbitrarily nonlinear, all harmonics could exist (i.e., none of q_n's vanishes). For example, if $q_h(t) = \cos(t) + \cos(2t)$, then this happens, and the fundamental frequency of $\dot{q}_h q_h$ is in fact 1, not 2, just like that of $\dot{q}_h$ (which corresponds to linear resonance). However, parametric resonance is often more prominent than linear resonance, measured in terms of peak sharpness (defined in subsection 4.2) for some special models, and we will see this numerically.

Remark 3.2. For the multidimensional case (e.g., $f(q,t)_j = A_j\cos(\Omega t)q_j$), by applying Theorem 2.7 and Example 2.8, the change of transition rate is expressed by $\delta S_e = -2|\sum_{j=1}^{nd} A_j \int_{-\infty}^{\infty} \dot{q}_h^j(t) q_h^j(t) e^{i\Omega t} dt|$, where $q_h^j(t)$ (resp., $\dot{q}_h^j(t)$) denotes the jth component of $q_h(t)$ (resp., $\dot{q}_h(t)$). As in (3.1), we further express $q_h^j(t)$ and $\dot{q}_h^j(t)$ as modulated Fourier series for $j = 1, \ldots, nd$. After substitution into δS_e, we can conduct estimation on integral δS_e to understand the resonant frequency of parametric resonance. Different from the single particle case, i.e., $n = d = 1$, Hess$V(x_a)$ will have multiple eigenvalues, and each will give a possible resonant frequency (the strength of each depends on the detailed interactions of coefficients, which is problem dependent, and hence no general claim will be stated). This will be verified numerically.

4. Experimental results. We now perform numerical experiments on specific models to illustrate our theoretical results.

4.1. Example 1: Double-well potential. As a first test, consider a single particle q moving in a 1-dimensional potential $V(q) = \frac{(1-q^2)^2}{4}$. For this example, $n = d = 1, \Gamma = \gamma$. The potential $V(q)$ has two wells of equal depth, situated at

$q_a = -1$, $q_b = 1$. A saddle point exists at $q_u = 0$. We use this example to explore the effect of parametric forcing $f(q,t) = A\cos(\Omega t)q$ on the metastable transition rate from q_a to q_b in light of Example 2.8.

Parametric resonance. We first approximate the heteroclinic orbit of the forceless system by numerically solving the uphill equation (2.20). More precisely, we take the time-reversed uphill equation with a sign flip on velocity and simulate the ODE. Since this is a second-order boundary value problem and the boundary points at $t = \pm\infty$ incur numerical difficulty, we make an approximation by choosing an initial q, p infinitesimally away from the saddle point, in the direction of the stable eigenvector of the uphill vector field linearized at the saddle $q_u = 0$, then simulate an initial value problem using fourth-order Runge–Kutta for long enough with a sufficiently small time step, and finally collect the result backward in time. Figure 1(a) shows an obtained heteroclinic connection from $q_a = -1$ to $q_u = 0$ with friction coefficient $\gamma = 0.1$ in phase space. Since q_a is a fixed point, the path circles around it for an arbitrarily long time.

With the unforced heteroclinic orbit, now we can examine the dependence of δS_e on input frequency Ω. For convenience, denote $|\int_{-\infty}^{\infty} \dot{q}_h(t) q_h(t) e^{i\Omega t} dt|$ by $|I(\Omega)|$. For each Ω, we compute $|I(\Omega)|$ by numerically approximating the integral via piecewise trapezoidal quadrature with high enough resolution. Figure 1(b) shows the relationship between the leading-order correction to action $|I(\Omega)|$ and Ω for parameter $\gamma = 0.1$. We observe that there exists special ω^* at which $|I(\Omega)|$ peaks, corresponding to the resonant frequency in our theoretical discussion. More details now follow.

Parametric resonant frequency. By the theoretical analysis conducted in section 3, the exact parametric resonant frequency is intrinsic frequency $\omega_0 = \sqrt{V''(q_a)} \approx 1.414$, with which heteroclinic orbit $q_h(t)$ oscillates around metastable state q_a. Consistent with this, as shown in Figure 1(b), the function $|I(\Omega)|$ displays a sharp peak near ω_0, and sequentially weaker peaks near its integer multiples. This is numerical evidence that the resonant frequencies are related to the intrinsic frequence ω_0 of the unperturbed system (2.20).

Estimation of $I(\Omega)$ near a resonant frequency. We proceed to depict the dependence of $|I(\Omega)|$ on Ω with γ fixed as $\gamma = 0.1,\ 0.01,\ 0.001$, which is shown in Figure 1(c). As we can see, smaller values of γ lead to more prominent peaks; i.e., near resonant frequency $\omega^* = \omega_0$, the value of $|I(\omega^*)|$ is larger when γ decreases. One can further find that $|I(\omega^*)|$ increases by a factor of 3.2160 when γ varies from 0.1 to 0.01 or a factor of 3.33 from 0.01 to 0.001 by comparing values of $|I(\omega^*)|$ (marked in Figure 1(c) with arrows) corresponding to $\gamma = 0.1, 0.01, 0.001$. Interestingly, such a numerical relation between $|I(\omega^*)|$ and γ satisfies $I(\omega^*) \sim \sqrt{\frac{1}{\gamma}} K$ approximately. This scaling with γ agrees well with our stationary phase estimate (3.5).

4.2. Example 2: Nonlinear pendulum (periodic potential). To further test our theoretical results, we now consider an even more nonlinear potential, $V(q) = \sin q$. Here $n = d = 1$. We will also use this example to illustrate the differences between linear resonance and parametric resonance.

Focusing on a compact neighborhood in which this potential has two local minima located in $q_a = -\frac{\pi}{2}$, $q_b = \frac{3}{2}\pi$, a saddle point located in $q_u = \frac{\pi}{2}$ separates their basins of attraction. Consider the two special forms of forcing $f(q,t)$ discussed in Example 2.8, the first being a linear forcing $f(t) = A\cos(\Omega t)$ and the second being a parametric forcing $f(q,t) = A\cos(\Omega t)q$.

In order to compare quantitatively, let us introduce the notion of peak sharpness, which is defined as the change ratio of $S_e(\Omega)$ in Ω, namely,

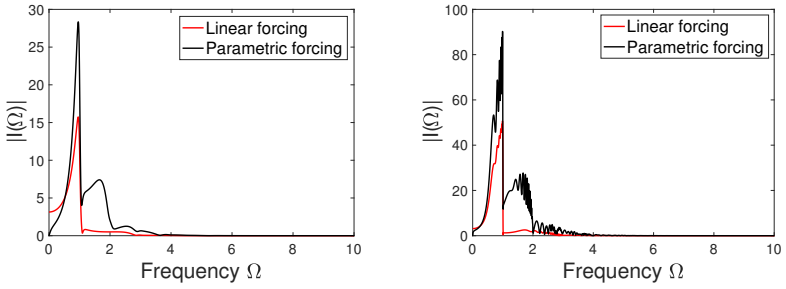

FIG. 2. *(Color online)* $\delta S = -2A\epsilon|I(\Omega)|$. *The dependence of action correction* $|I(\Omega)|$ *of system on frequency* Ω *in two special cases, respectively.* (a) *damping* $\gamma = 0.1$, (b) *damping* $\gamma = 0.01$.

TABLE 1
Values of peak sharpness.

Infinitesimal increment	Cases	$\rho_p(\omega^*)$	$\rho_l(\omega^*)$
	$\gamma = 0.1$	1.0118	1.0094
$d\Omega$=0.01	$\gamma = 0.01$	2.0212	1.2706
	γ=0.1	1.0077	1.0060
$d\Omega = -0.01$	γ=0.01	1.3957	1.0657

$$\rho_p(\Omega) = \frac{\left|\int_{-\infty}^{\infty} \dot{q}_h(t) q_h(t) e^{i\Omega t} dt\right|}{\left|\int_{-\infty}^{\infty} \dot{q}_h(t) q_h(t) e^{i(\Omega+d\Omega)t} dt\right|}, \quad \rho_l(\Omega) = \frac{\left|\int_{-\infty}^{\infty} \dot{q}_h(t) e^{i\Omega t} dt\right|}{\left|\int_{-\infty}^{\infty} \dot{q}_h(t) e^{i(\Omega+d\Omega)t} dt\right|}, \tag{4.1}$$

where $d\Omega$ is an infinitesimal increment. If $\rho_p(\omega^*) > \rho_l(\omega^*)$ holds, it means that parametric excitation at a resonant frequency leads to a sharper peak than that of linear excitation, and we utilize it as a basis to check if parametric resonance is more apparent than linear resonance.

As in subsection 4.1, numerically computed $|I(\Omega)|$ for $\gamma = 0.1, 0.01$ is plotted in Figure 2, respectively. Again, the main peaks of $|I(\Omega)|$ correspond to intrinsic frequency $\omega^* \approx \omega_0 \approx 1$, both in the case of additive and parametric forcing. In terms of (4.1), we can compute $\rho_l(\omega^*)$, $\rho_p(\omega^*)$ both for $d\Omega = 0.01,\ -0.01$ and $\gamma = 0.1,\ 0.001$ and list them in Table 1. According to these data, it is interesting to see that the peak of parametric resonance is sharper. One can further find that $\rho_p(\omega^*)$ varies more greater than that of $\rho_l(\omega^*)$ as γ decreases from 0.1 to 0.01. The results in this example seem to suggest that parametric resonance is often more prominent than linear resonance in terms of peak sharpness.

4.3. Example 3: Lennard–Jones molecular cluster. Finally, let us consider a practical application, for which we apply our techniques to a multiparticle molecular system. Based on Theorem 2.7, Example 2.8, and Remark 3.2, we now characterize the parametric resonant frequency in a higher-dimensional case numerically.

We consider $n = 36$ molecules in a $d = 2$-dimensional periodic box (with box sizes $s_x = 3\sqrt{3}$, $s_y = 6$ in x- and y-directions, respectively). The jth molecule's location is denoted by $q^{(j)} = (x^{(j)}, y^{(j)})^T \in (\mathbb{R}/s_x) \times (\mathbb{R}/s_y)$. The governing dynamics is

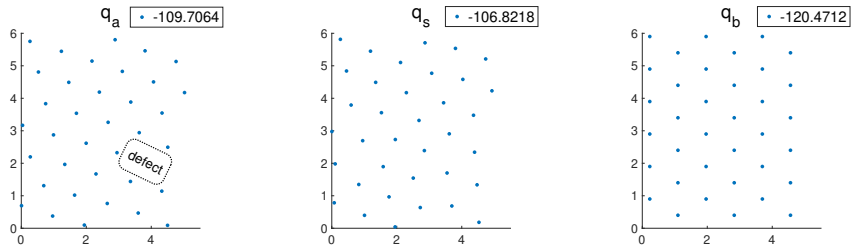

(a) (b) (c)

FIG. 3. *(Color online) Configurations and corresponding potential values:* $r_0 = 1$. (a) *Initial configuration (defective metastable state—one can see there is vacancy in the defective area and atoms nearby deviated from perfect lattice),* (b) *saddle configuration, and* (c) *final configuration (perfect lattice metastable state).*

$$\begin{aligned} \ddot{x}^{(j)} + \gamma \dot{x}^{(j)} &= -\frac{\partial}{\partial x^{(j)}} V_{LJ}(\cdot) + \varepsilon A_1 \cos(\omega t) x^{(j)} + \sqrt{\mu}\gamma^{\frac{1}{2}} \xi_x^{(j)}(t), \\ \ddot{y}^{(j)} + \gamma \dot{y}^{(j)} &= -\frac{\partial}{\partial y^{(j)}} V_{LJ}(\cdot) + \varepsilon A_2 \cos(\omega t) y^{(j)} + \sqrt{\mu}\gamma^{\frac{1}{2}} \xi_y^{(j)}(t) \end{aligned} \tag{4.2}$$

for $j = 1, \ldots, 36$. The parametric form of the forcing is inspired by the classical Hamiltonian approximation of charged particles in the external time-varying electric field, which is popular in modeling laser-controlled molecules (e.g., [38]). We use the notation

$$r_{ij} = \left(\left| \operatorname{mod}\left(x^{(i)} - x^{(j)} + \frac{s_x}{2}, s_x \right) - \frac{s_x}{2} \right|^2 + \left| \operatorname{mod}\left(y^{(i)} - y^{(j)} + \frac{s_y}{2}, s_y \right) - \frac{s_y}{2} \right|^2 \right)^{\frac{1}{2}}$$

to denote the distance between the ith and jth molecules under the periodic boundary condition (i.e., geodesic distance on the 2-torus). V_{LJ} is a Lennard–Jones potential which is widely used in molecular modeling, and it is the sum of pairwise interactions, $V_{LJ}(r) = \sum_{i \neq j, i, j=1}^{n} [(\frac{r_0}{r_{ij}})^{12} - 2(\frac{r_0}{r_{ij}})^6]$, where r_0 is a constant parameter denoting the characteristic distance of particles, which is taken as $r_0 = 1$ here. This potential has a lot of local minima, and for an important material sciences application, we consider a global minimum q_b corresponding to a perfect lattice configuration and a local minimum q_a corresponding to material with a local defect, and we are interested in how to turn the material from the defective state q_a to the perfect state q_b. In addition, there is a saddle point at q_s on the separatrix between q_a and q_b, and these fixed points are depicted in Figure 3. At the minima $V(q_a) \approx -109.7064$, $V(q_b) \approx -120.4712$, and at the saddle point $V(q_s) \approx -106.8218$. In this case, increasing the metastable transition rate from q_a to q_b is of particular importance, as it corresponds to healing the defect of the material. This transition is still a rare event, but we will see its likelihood can be significantly increased by an appropriate homogeneous external vibration (i.e., shaking the material to perfect its lattice).

For the case of parametric perturbation discussed here, by applying Theorem 2.7 and Example 2.8, the change of the transition rate from q_a to q_b is given by a more simple form:

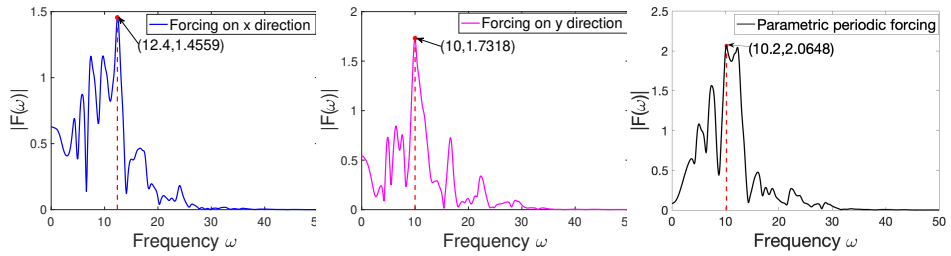

(a) (b) (c)

FIG. 4. *(Color online)* $\delta S_e = -2A|F(\omega)|$*: damping* $\gamma = 1$*. The dependence of action correction* $|F(\omega)|$ *of* (4.2) *on frequency* ω *in three special cases, respectively.*

$$\delta S_e = \begin{cases} -2A_1 \left| \sum_{j=1}^{n} \int_{-\infty}^{\infty} \dot{x}^{(j)}(t) x^{(j)}(t) e^{i\omega t} dt \right| & \text{if } A_1 \neq 0,\ A_2 = 0, \\ -2A_2 \left| \sum_{j=1}^{n} \int_{-\infty}^{\infty} \dot{y}^{(j)}(t) y^{(j)}(t) e^{i\omega t} dt \right| & \text{if } A_1 = 0,\ A_2 \neq 0, \\ -2A \left| \sum_{j=1}^{n} \int_{-\infty}^{\infty} \left(\dot{x}^{(j)}(t) x^{(j)}(t) + \dot{y}^{(j)}(t) y^{(j)}(t) \right) e^{i\omega t} dt \right| & \text{if } A_1 = A_2 = A \neq 0. \end{cases}$$

As in subsection 4.1, let us first compute the heteroclinic connection (2.20) from q_a to q_s numerically. Then the application we need to do is to find the optimal frequency ω^*, vibrating q_a into q_b through q_s, to achieve the purpose of healing the defect.

Parametric resonant frequency. For simplicity, let $|F(\omega)|$ denote the $|\cdot|$ part in the above formula. We numerically computed the heteroclinic orbit in the unforced system, which gives $x, y, \dot{x}, \dot{y}$, and then evaluate $|F(\omega)|$ via quadrature over a range of ω values. The results of the three different parametric forcing cases, respectively, corresponding to vibrating in the x- and y-direction and both directions, are plotted in Figure 4 for damping coefficient $\gamma = 1$.

We again see that $|F(\omega)|$ displays clear peaks. Different from the problems of a single particle in one dimension, $\mathrm{Hess}V(q_a)$ is now a 72×72 matrix with multiple eigenvalues instead of just one. By examining the list of eigenvalues, we see that resonant frequencies again coincide with eigenvalues of the matrix $\mathrm{Hess}V(q_a)$. The strongest resonant frequency is marked in each plot. Therefore, to heal a defective material, one possibility is to use our theory and compute the resonant frequencies and then try vibrations at those frequencies. Of course, given this is a high-dimensional system, there are many different ways to combine vibrations at each dimension; if one wants to optimize the combination, our theory can also help, and one no longer has to conduct computationally expensive rare event simulations, but this becomes an optimization problem which deserves an adequate investigation in a different study.

Comparison to linear forcing. The rest of this subsection is devoted to a comparison to the case of linear perturbation; a clear advantage of parametric forcing will be illustrated. Specifically, the governing dynamics for the case of linear perturbation is

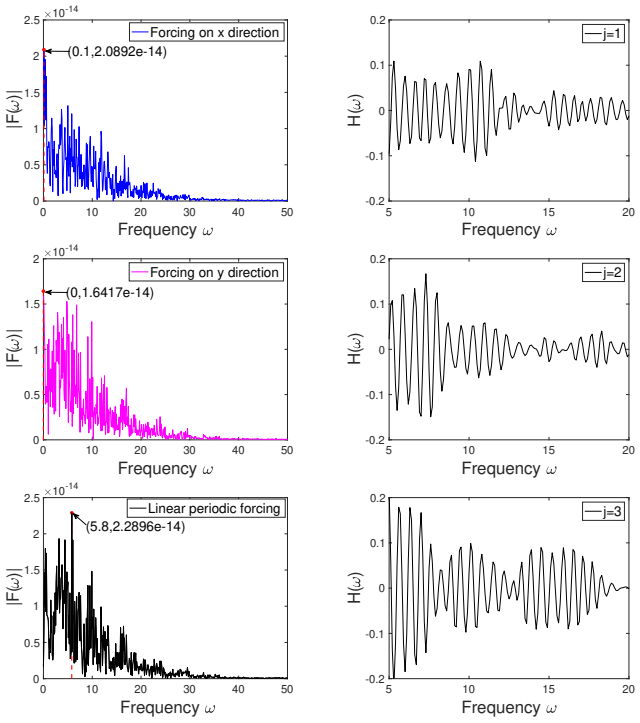

FIG. 5. *(Color online) Damping* $\gamma = 1$. (a) $\delta S_e = -2A\epsilon|F(\omega)|$. *The dependence of action correction* $|F(\omega)|$ *on frequency* ω *in three special linear forcing cases, respectively.* (b) *The dependence of components* $Re[\int_{-\infty}^{\infty} \dot{x}^{(j)}(t)e^{i\omega t}dt]$ *denoted by* $H(\omega)$ *on frequency* ω *for* $j = 1, 2, 3$. *Note we zoomed in on the x-axis for improved readability. This is reasonable since we just need to show the cancellation here and the plots need not to be very complete.*

$$\begin{aligned} \ddot{x}^{(j)} + \gamma\dot{x}^{(j)} &= -\frac{\partial}{\partial x^{(j)}}V_{LJ}(\cdot) + \varepsilon A_1\cos(\omega t) + \sqrt{\mu}\gamma^{\frac{1}{2}}\xi_x^{(j)}(t), \\ \ddot{y}^{(j)} + \gamma\dot{y}^{(j)} &= -\frac{\partial}{\partial y^{(j)}}V_{LJ}(\cdot) + \varepsilon A_2\cos(\omega t) + \sqrt{\mu}\gamma^{\frac{1}{2}}\xi_y^{(j)}(t) \end{aligned} \tag{4.3}$$

for $j = 1, \ldots, 36$. Again, the change of the transition rate from q_a to q_b is written in a more simple form: $\delta S_e = -2A_1|\sum_{j=1}^{n}\int_{-\infty}^{\infty}\dot{x}^{(j)}(t)e^{i\omega t}dt|$ or $-2A_2|\sum_{j=1}^{n}\int_{-\infty}^{\infty}\dot{y}^{(j)}(t)e^{i\omega t}dt|$ if one of A_1, A_2 is zero and another is nonzero; otherwise, i.e., $A_1 = A_2 = A \neq 0$, $\delta S_e = -2A|\sum_{j=1}^{n}\int_{-\infty}^{\infty}(\dot{x}^{(j)}(t) + \dot{y}^{(j)}(t))e^{i\omega t}dt|$ based on Theorem 2.7 and Example 2.8.

Let $|F(\omega)|$ still denote the $|\cdot|$ part in the above formula. The frequency response results of the three different linear forcing cases, respectively, corresponding to vibrations in the x- and y-direction and both directions, are plotted in Figure 5(a) for damping coefficient $\gamma = 1$. One may again try to identify special w^* values at which $|F(\omega)|$ peaks, but these peaks are not as well defined as those in the parametric resonance case. In fact, note the drastic difference between $|F|$ values in the parametric case (~ 1) and this (linear) case ($\sim 10^{-14}$). We feel there is no strong resonance in this case anymore, and integrals cancel out so that the computed δS_e is dominated by (small) numerical errors. To illustrate this cancellation, the plots of $Re[\int_{-\infty}^{\infty}\dot{x}^{(j)}(t)e^{i\omega t}dt]$ (denoted by $H(\omega)$) as functions of ω for several different j's are also provided in Figure 5(b).

This is empirical evidence of the advantage of parametric excitation; at least it leads to resonant enhancement of the recovery of material defect.

5. Conclusion. In this work, we derived a closed-form explicit expression that characterizes how a small, generic nonlinear periodic forcing affects the metastable transition rate in kinetic Langevin systems of arbitrary dimensions. This is done by viewing the high-order Euler–Lagrange equations associated with the Freidlin–Wentzell action minimization in the perspective of perturbed Hamiltonian dynamics. Perturbation analysis allows the MLP and its rate to be approximated from the heteroclinic connection in the unperturbed, noiseless system. Furthermore, we showed that parametric periodic perturbation facilitates metastable transitions by theoretically characterizing the resonant frequency of parametric excitation via stationary phase asymptotics. Numerical experiments for both low-dimensional toy models and a 144-dimensional molecular cluster validated our theory. The method we developed here could offer insights into the interaction between periodic force and noise in rather general systems.

Acknowledgments. The authors thank Prof. Maria Cameron, Prof. Wang Sang Koon, Prof. Jinqiao Duan, and Dr. Pingyuan Wei for helpful discussions. This work was primarily done while Y.C. was a visiting scholar at Georgia Institute of Technology.

REFERENCES

[1] N. Agudov and B. Spagnolo, *Noise-enhanced stability of periodically driven metastable states*, Phys. Rev. E, 64 (2001), 035102.
[2] M. Assaf, A. Kamenev, and B. Meerson, *Population extinction in a time-modulated environment*, Phys. Rev. E, 78 (2008), 041123.
[3] A. Assion, T. Baumert, M. Bergt, T. Brixner, B. Kiefer, V. Seyfried, M. Strehle, and G. Gerber, *Control of chemical reactions by feedback-optimized phase-shaped femtosecond laser pulses*, Science, 282 (1998), pp. 919–922.
[4] L. Billings and E. Forgoston, *Seasonal forcing in stochastic epidemiology models*, Ric. Mat., 67 (2018), pp. 27–47.
[5] F. Bouchet and J. Reygner, *Generalisation of the Eyring–Kramers transition rate formula to irreversible diffusion processes*, Ann. Henri Poincaré, 17 (2016), pp. 3499–3532.
[6] T. Brixner, N. Damrauer, P. Niklaus, and G. Gerber, *Photoselective adaptive femtosecond quantum control in the liquid phase*, Nature, 414 (2001), pp. 57–60.
[7] M. Cameron and S. Yang, *Computing the quasipotential for highly dissipative and chaotic SDEs an application to stochastic Lorenz'63*, Commun. Appl. Math. Comput. Sci., 14 (2019), pp. 207–246.
[8] M. Capinski and P. Zgliczynski, *Beyond the Melnikov Method* II: *Multidimensional Setting*, preprint, arXiv:1803.01587, 2018.
[9] Y. Chen, J. Gemmer, M. Silber, and A. Volkening, *Noise-induced tipping under periodic forcing: Preferred tipping phase in a non-adiabatic forcing regime*, Chaos, 29 (2019), 043119.
[10] Z. Chen, Y. Li, and X. Liu, *Noise induced escape from a nonhyperbolic chaotic attractor of a periodically driven nonlinear oscillator*, Chaos, 26 (2016), 063112.
[11] D. Dahiya and M. Cameron, *An ordered line integral method for computing the quasi-potential in the case of variable anisotropic diffusion*, Phys. D, 382 (2018), pp. 33–45.
[12] D. Dahiya and M. Cameron, *Ordered line integral methods for computing the quasi-potential*, J. Sci. Comput., 75 (2018), pp. 1351–1384.
[13] C. Daniel, J. Full, L. González, C. Lupulescu, J. Manz, A. Merli, Š. Vajda, and L. Wöste, *Deciphering the reaction dynamics underlying optimal control laser fields*, Science, 299 (2003), pp. 536–539.
[14] A. Dembo and O. Zeitouni, *Large Deviations Techniques and Applications*, Springer, New York, 2010.
[15] A. Dubkov, N. Agudov, and B. Spagnolo, *Noise enhanced stability in fluctuating metastable states*, Phys. Rev. E, 69 (2004), 61103.

[16] M. Dykman, B. Golding, L. Mccann, V. Smelyanskiy, D. Luchinsky, R. Mannella, and P. Mcclintock, *Activated escape of periodically driven systems*, Chaos, 11 (2001), pp. 587–594.
[17] M. Dykman, H. Rabitz, V. Smelyanskiy, and B. Vugmeister, *Resonant directed diffusion in nonadiabatically driven systems*, Phys. Rev. Lett., 79 (1997), pp. 1178–1181.
[18] C. Escudero and J. Rodríguez, *Persistence of instanton connections in chemical reactions with time-dependent rates*, Phys. Rev. E, 77 (2008), 011130.
[19] E. Forgoston and R. O. Moore, *A primer on noise-induced transitions in applied dynamical systems*, SIAM Rev., 60 (2018), pp. 969–1009.
[20] M. Freidlin and A. Wentzell, *Random Perturbations of Dynamical Systems*, Springer, New York, 2012.
[21] L. Gammaitoni, P. Hänggi, P. Jung, and F. Marchesoni, *Stochastic resonance*, Rev. Modern Phys., 70 (1998), pp. 223–287.
[22] T. Grafke, R. Grauer, and T. Schäfer, *The instanton method and its numerical implementation in fluid mechanics*, J. Phys. A, 48 (2015), 333001.
[23] T. Grafke, T. Schäfer, and E. Vanden-Eijnden, *Long term effects of small random perturbations on dynamical systems: Theoretical and computational tools*, in Recent Progress and Modern Challenges in Applied Mathematics, Modeling and Computational Science, Springer, New York, 2017, pp. 17–55.
[24] J. Guckenheimer and P. Holmes, *Nonlinear Oscillations, Dynamical Systems, and Bifurcations of Vector Fields*, Springer, New York, 1983.
[25] M. Heymann and E. Vanden-Eijnden, *The geometric minimum action method: A least action principle on the space of curves*, Comm. Pure Appl. Math., 61 (2008), pp. 1052–1117.
[26] M. Heymann and E. Vanden-Eijnden, *Pathways of maximum likelihood for rare events in nonequilibrium systems: Application to nucleation in the presence of shear*, Phys. Rev. Lett., 100 (2008), 140601.
[27] R. Judson and H. Rabitz, *Teaching lasers to control molecules*, Phys. Rev. Lett., 68 (1992), 1500.
[28] P. Jung and P. Hänggi, *Amplification of small signals via stochastic resonance*, Phys. Rev. A, 44 (1991), pp. 8032–8042.
[29] P. Kapitza, *Dynamic stability of the pendulum with vibrating suspension point*, Sov. Phys. JETP, 21 (1951), pp. 588–597.
[30] I. Khovanov, A. Polovinkin, D. Luchinsky, and P. McClintock, *Noise-induced escape in an excitable system*, Phys. Rev. E, 87 (2013), 032116.
[31] W. Koon, H. Owhadi, M. Tao, and T. Yanao, *Control of a model of DNA division via parametric resonance*, Chaos, 23 (2013), 013117.
[32] R. Levis, G. Menkir, and H. Rabitz, *Selective bond dissociation and rearrangement with optimally tailored, strong-field laser pulses*, Science, 292 (2001), pp. 709–713.
[33] B. Lin, Q. Li, and W. Ren, *A Data Driven Method for Computing Quasipotentials*, preprint, arXiv:2012.09111, 2020.
[34] L. Lin, H. Yu, and X. Zhou, *Quasi-potential calculation and minimum action method for limit cycle*, J. Nonlinear Sci., 29 (2019), pp. 961–991.
[35] B. S. Lindley and I. B. Schwartz, *An iterative action minimizing method for computing optimal paths in stochastic dynamical systems*, Phys. D, 255 (2013), pp. 22–30.
[36] V. Lucarini, *Stochastic resonance for nonequilibrium systems*, Phys. Rev. E, 100 (2019), 062124.
[37] R. Maier and D. Stein, *Noise-activated escape from a sloshing potential well*, Phys. Rev. Lett., 86 (2001), pp. 3942–3945.
[38] F. Mauger, C. Chandre, and T. Uzer, *Recollisions and correlated double ionization with circularly polarized light*, Physical Review Letters, 105 (2010), 083002.
[39] J. Meiss, *Differential Dynamical Systems*, Math. Model. Comput. 14, SIAM, Philadelphia, 2007.
[40] V. Melnikov, *On the stability of a center for time-periodic perturbations*, Trans. Moscow Math. Soc., 12 (1963), pp. 3–52.
[41] W. Paul, *Electromagnetic traps for charged and neutral particles (Nobel lecture)*, Angew. Chemie Intern. Ed. in English, 29 (1990), pp. 739–748.
[42] C. Presilla, F. Marchesoni, and L. Gammaitoni, *Periodically time-modulated bistable systems: Nonstationary statistical properties*, Phys. Rev. A, 40 (1989), pp. 2105–2113.
[43] F. Ragone, J. Wouters, and F. Bouchet, *Computation of extreme heat waves in climate models using a large deviation algorithm*, Proc. Natl. Acad. Sci. USA, 115 (2018), pp. 24–29.
[44] F. Riahi, *On lagrangians with higher order derivatives*, Am. J. Phys., 40 (1972), pp. 386–390.

[45] S. Rice and M. Zhao, *Optical Control of Molecular Dynamics*, AIP Publishing, Melville, NY, 2000.
[46] M. Shapiro and P. Brumer, *Quantum Control of Molecular Processes*, John Wiley and Sons, Hoboken, NJ, 2012.
[47] V. Smelyanskiy, M. Dykman, H. Rabitz, and B. Vugmeister, *Fluctuations, escape, and nucleation in driven systems: Logarithmic susceptibility*, Phys. Rev. Lett., 79 (1997), pp. 3113–3116.
[48] A. Souza and M. Tao, *Metastable transitions in inertial Langevin systems: What can be different from the overdamped case?*, European J. Appl. Math., 30 (2019), pp. 830–852.
[49] S. Surappa, M. Tao, and F. L. Degertekin, *Analysis and design of capacitive parametric ultrasonic transducers for efficient ultrasonic power transfer based on a* $1D$ *lumped model*, IEEE T. Ultrason. Ferroelectr. Freq. Control, 65 (2018), pp. 2103–2112.
[50] M. Tao, *Hyperbolic periodic orbits in nongradient systems and small-noise-induced metastable transitions*, Phys. D, 363 (2018), pp. 1–17.
[51] M. Tao, *Simply improved averaging for coupled oscillators and weakly nonlinear waves*, Commun. Nonlinear Sci. Numer. Simul., 71 (2019), pp. 1–21.
[52] M. Tao and H. Owhadi, *Temporal homogenization of linear ODEs, with applications to parametric super-resonance and energy harvest*, Arch. Ration. Mech. Anal., 220 (2016), pp. 261–296.
[53] T. Tao, *Lecture Notes* 8 *for* 247*b*, University of California, Los Angles, 2022, http://www.math.ucla.edu/~tao/247b.1.07w/notes8.pdf.
[54] X. Wan, *An adaptive high-order minimum action method*, J. Comput. Phys., 230 (2011), pp. 8669–8682.
[55] E. Weinan, W. Ren, and E. Vanden-Eijnden, *String method for the study of rare events*, Phys. Rev. B, 66 (2002), 052301.
[56] E. Weinan, W. Ren, and E. Vanden-Eijnden, *Minimum action method for the study of rare events*, Comm. Pure Appl. Math., 57 (2004), pp. 637–656.
[57] P. Xie and M. Tao, *Parametric resonant control of macroscopic behaviors of multiple oscillators*, in Proceedings of the 2019 American Control Conference (ACC), IEEE, 2019.
[58] K. Yagasaki, *Heteroclinic transition motions in periodic perturbations of conservative systems with an application to forced rigid body dynamics*, Regul. Chaotic Dyn., 23 (2018), pp. 438–457.
[59] S. Yang, S. F. Potter, and M. K. Cameron, *Computing the quasipotential for nongradient SDES in* $3D$, J. Comput. Phys., 379 (2019), pp. 325–350.
[60] X. Zhou, W. Ren, and W. E, *Adaptive minimum action method for the study of rare events*, J. Chem. Phys., 128 (2008), 104111.